INTERLAMINAR FRACTURE TESTING OF MULTIDIRECTIONAL LAMINATES: ON FINITEWIDTH EFFECT AND RESIDUAL STRESSES

Torquato Garulli[1,2], Albertino Arteiro[3], Norbert Blanco[4] Villaverde and Jordi Renart Canalias[5]

[1]AMADE, Polytechnic School, University of Girona, Campus Montilivi s/n, 17071 Girona, Spain
[2]Department of Aeronautics, Imperial College London, South Kensington Campus, SW7 2AZ London, United Kingdom
Email: torquato.garulli@udg.edu
[3]DEMec, Faculty of Engineering, University of Porto, Rua Dr. Roberto Frias, s/n, 4200-465 Porto, Portugal
Email: aarteiro@fe.up.pt
[4]AMADE, Polytechnic School, University of Girona, Campus Montilivi s/n, 17071 Girona, Spain
Email: norbert.blanco@udg.edu
[5]AMADE, Polytechnic School, University of Girona, Campus Montilivi s/n, 17071 Girona, Spain
Email: jordi.renart@udg.edu

Keywords: Interlaminar fracture toughness, Fully-uncoupled Multidirectional specimens, Delamination, Residual stresses

Abstract
Fibre reinforced polymers, and in particular laminated plates, are widely used in structural applications. Interlaminar fracture (delamination) is a critical damage mechanism for these materials. Interlaminar fracture toughness is characterised using unidirectional specimens. While the toughness at interfaces in multidirectional laminates may be different, there is no consensus on how to effectively characterise it, due to a number of challenges associated with the use of multidirectional specimens. In this work, we review in detail some of these problems, namely, 3-dimensional effects and residual thermal stresses. We then present a strategy to design a set of Fully-Uncoupled Multidirectional specimens enabling a further understanding of these problems.

1. Introduction

Fibre Reinforced Polymers (FRPs) are extensively used in lightweight structures, due to their outstanding specific mechanical properties. Knowledge of their failure mechanisms and properties is essential to guarantee structural safety. Interlaminar fracture, also known as delamination, is one of the most threatening damage mechanisms occurring in laminated FRPs. Therefore, reliable characterization of interlaminar fracture toughness (IFT) is a major concern and is performed following international standards. All available standards suggest the use of unidirectional (UD) specimens, where delamination is propagated along the fibre direction. However, in real applications, multidirectional (MD) laminates are most often used, and delamination may initiate in interfaces between differently oriented layers and grow in any direction. Under these circumstances, IFT may be different from that measured in standard tests on UD specimens [1]. Nonetheless, strategies to characterize IFT in MD interfaces (i.e. between differently oriented layers) are still lacking. This stems from the problems encountered when using MD specimens [2], namely: three-dimensional (3D) effects, thermal residual stresses, additional energy dissipation mechanisms in off-axis plies, and delamination migration. For decades, researchers have tried to design MD specimens able to avoid/minimize these problems. A recent development was the introduction of Fully-Uncoupled Multi-Directional (FUMD) delamination specimens [3,4]. Preliminary

studies have shown the benefits of these specimens [5], making them viable candidates for standardisation purposes. In this study, we focus on 3D effects and on thermal residual stresses and we set out to design and analyse a set of FUMD delamination specimens that would enable evaluation of the effects of ply-level residual stresses on IFT.

2. Thermoelastic couplings and finite width effect in MD delamination specimens

2.1. Thermoelastic behaviour of composite laminates

The thermoelastic behaviour of composite laminates can be described using Classic Laminated Plate Theory (CLPT), which leads to the following constitutive equation:

$$\begin{Bmatrix} \{N\} \\ \{M\} \end{Bmatrix} = \begin{bmatrix} [A] & [B] \\ [B] & [D] \end{bmatrix} \begin{Bmatrix} \{\varepsilon^0\} \\ \{\chi\} \end{Bmatrix} - \Delta T \begin{Bmatrix} \{U\} \\ \{V\} \end{Bmatrix}. \tag{1}$$

In Eq. (1), $\{N\}$ and $\{M\}$ are the vectors of in-plane force resultants and of moment resultants, respectively; $\{\varepsilon^0\}$ and $\{\chi\}$ are the vectors of midplane strains and curvatures, respectively; $\{U\}$ and $\{V\}$ are respectively the vectors of thermal force and moment resultants per unit temperature change, ΔT being the temperature change from an unstrained reference temperature; $[A]$, $[B]$, and $[D]$ are the extensional stiffness matrix, the bending-extension coupling matrix and the bending stiffness matrix of the laminate, respectively. Eq. (1) can be inverted to obtain:

$$\begin{Bmatrix} \{\varepsilon^0\} \\ \{\chi\} \end{Bmatrix} = \begin{bmatrix} [a] & [b] \\ [b]^T & [d] \end{bmatrix} \begin{Bmatrix} \{N\} \\ \{M\} \end{Bmatrix} + \Delta T \begin{Bmatrix} \{\alpha^\varepsilon\} \\ \{\alpha^\chi\} \end{Bmatrix}, \tag{2}$$

where $\{\alpha^\varepsilon\}$ and $\{\alpha^\chi\}$ are the vectors of the laminate effective coefficients of thermal expansion (CTEs):

$$\begin{Bmatrix} \{\alpha^\varepsilon\} \\ \{\alpha^\chi\} \end{Bmatrix} = \begin{bmatrix} [a] & [b] \\ [b]^T & [d] \end{bmatrix} \begin{Bmatrix} \{U\} \\ \{V\} \end{Bmatrix}. \tag{3}$$

For later convenience, Eq. (2) may be written in explicit form as:

$$\begin{Bmatrix} \varepsilon_x^0 \\ \varepsilon_y^0 \\ \varepsilon_{xy}^0 \\ \chi_x \\ \chi_y \\ \chi_{xy} \end{Bmatrix} = \begin{bmatrix} a_{11} & a_{12} & a_{16} & b_{11} & b_{12} & b_{16} \\ a_{12} & a_{22} & a_{26} & b_{21} & b_{22} & b_{26} \\ a_{16} & a_{26} & a_{66} & b_{61} & b_{62} & b_{66} \\ b_{11} & b_{21} & b_{61} & d_{11} & d_{12} & d_{16} \\ b_{12} & b_{22} & b_{62} & d_{12} & d_{22} & d_{26} \\ b_{16} & b_{26} & b_{66} & d_{16} & d_{26} & d_{66} \end{bmatrix} \begin{Bmatrix} N_x \\ N_y \\ N_{xy} \\ M_x \\ M_y \\ M_{xy} \end{Bmatrix} + \Delta T \begin{Bmatrix} \alpha_x^\varepsilon \\ \alpha_y^\varepsilon \\ \alpha_{xy}^\varepsilon \\ \alpha_x^\chi \\ \alpha_y^\chi \\ \alpha_{xy}^\chi \end{Bmatrix}. \tag{4}$$

2.2. Thermoelastic couplings

Thermoelastic couplings of composite laminates are represented in Eq. (4) by the following terms:
- a_{16} and a_{26}, constituting stretching-shearing coupling (also called in-plane couplings);
- b_{11}, b_{22}, b_{12} and b_{21}, constituting stretching-bending coupling;
- b_{16} and b_{26}, constituting stretching-twisting coupling;
- b_{61} and b_{62}, constituting shearing-bending coupling;
- b_{66}, constituting shearing-twisting coupling;
- d_{16} and d_{26}, constituting bending-twisting coupling;
- α_{xy}^ε, α_x^χ, α_y^χ, and α_{xy}^χ, constituting coupling between thermal load and elastic deformation.

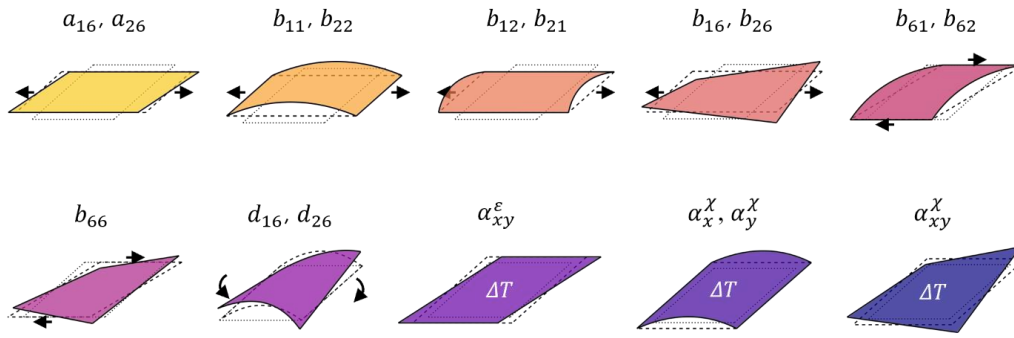The effects induced by these terms are schematically illustrated in Figure 1.

Figure 1. Representation of the effects induced by thermoelastic couplings.

Ideally, a 2D state (plane stress or plane strain) of the specimen arms would be sought. Couplings complicate the kinematics of the specimen, introducing undesired deformation and stress components, leading to undesired modal contributions to the energy release rate (ERR) along the delamination front. Additionally, couplings may lead to an unsymmetric distribution of ERR along the delamination front, which in turn may lead to uneven propagation and hence to a skewed delamination front. Hence, thermoelastic couplings should be minimised or eliminated [6]. Historically, the greatest focus has been on the bending-twisting coupling, and the nondimensional ratio B_t [7], defined in Eq. (5) has been widely used, as a parameter to be minimised for each of the specimen arms.

$$B_t = \left| \frac{D_{16}}{D_{11}} \right| \tag{5}$$

2.3. Finite width effects
Even if all the thermoelastic couplings described above were avoided, 3D effects still arise due to the specimen finite width. In fact, the stress state in the specimen arms depends on their elastic properties and on their aspect ratio (ratio between precrack length and specimen width). Davidson and colleagues demonstrated that the difference in mechanical behaviour (i.e. deflection) between plane stress and plane strain conditions is related to the nondimensional parameter D_c [8], that can be obtained as:

$$D_c = \frac{D_{12}^2}{D_{11} D_{22}} . \tag{6}$$

Low D_c values mean that only minor differences exist between plane stress and plane strain conditions. UD specimens have low values of D_c. Consequently, changes in the aspect ratio will have negligible effect on the mechanical behaviour of the specimen. On the contrary, high Dc values, as may be found for MD specimens, indicate large differences between plane stress and plane strain conditions; also, they are associated with large aspect ratio intervals for which a specimen is neither under plane stress nor plane strain conditions [8]. This may lead to errors if data reduction procedures not including any strategy to account for finite width are used. Furthermore, during the test, the aspect ratio will change, thus changing the specimen stress state and leading to non-self-similar propagation, which again may introduce errors in the evaluation of IFT [8]. It can be noted D_c is related to the stiffness term D_{12}, which measures the anticlastic behaviour of the laminate: high D_c values mean a strong anticlastic effect, which leads to an uneven ERR distribution at the delamination front, and thus to curved delamination fronts.

2.4. Thermal residual stresses
Thermal residual stresses in composite laminates develop due to different mechanisms at different length scales. While the overall residual stress state will depend upon all mechanisms together, it is convenient, for simplicity, to describe them separately. In the following, we consider thermoset matrix composites.

At the microscale, *micro* residual stresses develop due to chemical shrinkage of the resin during curing and due to the different fibres and matrix CTEs during the subsequent cooling. Nairn suggested that these stresses do not contribute to ERR if UD specimens are used [9], while their contribution to ERR in MD specimens has not been clarified. These stresses depend on material properties and processing conditions and might be not influenced by the stacking sequence. Nonetheless, micromechanical studies revealed that they can affect strength properties [10], which may be important for MD specimens, as it may facilitate delamination migration and undesired dissipation mechanisms. Moreover, micro residual stresses may constitute a significant portion of the overall residual stresses in a MD laminate [11].

At a larger scale, when a laminate cools after processing, it will shrink according to its CTEs. These are functions of the ply material and of the stacking sequence; in other words, the laminate shrinks in a way that averages the behaviour of all its plies. When each ply is considered individually, its CTEs will be, in general, different from the laminate ones (except for UD laminates). Consequently, during cooling the ply will be constrained to deform according to the overall laminate contraction, rather than to its own CTEs, which causes ply-level residual stresses to develop. Numerical and experimental studies suggest that these stresses may not affect the load displacement behaviour of MD specimen, but they may facilitate delamination migration [12,13]. These stresses may be estimated, as a first approximation, using CLPT. For a given ply, the ply-level residual stresses in laminate coordinates can be obtained as:

$$\{\sigma\} = [\bar{Q}]\Delta T\big((\{\alpha^\varepsilon\} - z\{\alpha^\chi\}) - \{\bar{\alpha}\}\big), \tag{7}$$

where $[\bar{Q}]$ is the ply reduced stiffness matrix and $\{\bar{\alpha}\}$ the vector of ply CTEs, both expressed in laminate coordinates; z is the coordinate in the laminate thickness direction. In Eq. (7), the term inside the innermost parentheses correspond to the ply residual strain, written as a function of the laminate CTEs and where ΔT has been taken out as a factor; it clearly shows how the ply residual strain is dictated by the overall laminate contraction. Hence, the content of the outermost parentheses shows that ply-level residual stresses arise due to a difference between the residual strain imposed on a ply by the laminate contraction and the strain the ply would undergo if not constrained, according to its own CTEs, $\{\bar{\alpha}\}$.

3. Specimens design strategies

3.1. General considerations and strategies

Historically, D_c and B_t have been used as the main design parameters, consensus being that they should be as low as possible for both specimen arms. Minimisation of D_c is achieved including a high number of 0º plies in the layup, but the concurrent minimisation of D_c and B_t has proven challenging [7,14]. Furthermore, recent numerical results [3,4] suggest that even when a specimen has low D_c and B_t for each arm, undesired effects may exist if the arms have different elastic properties [3,4].

Concerning ply-level residual stresses, Eq. (7) shows that they depend upon the ply orientation and its position (z) in the laminate; furthermore, they are governed by the laminate CTEs, that in turn show a cumbersome dependence on the stacking sequence (through, $\{U\}$, $\{V\}$, and the inverted of the [ABD] matrix), Eq. (3). Nairn suggested that doubly-symmetric (i.e. symmetric and in which both halves are symmetric) sequences be used to avoid errors in IFT evaluation [15]. Thus, no residual curvature develops in either arm or in the uncracked region. However, each ply will still develop residual stresses, and experimental evidence suggests that changing these stresses leads to changes in the measured IFT [16]. Furthermore, this strategy severely limits the design space and restrict the delaminating interface to be in between plies with the same orientation. A better understanding of the effect of ply-level residual stresses and better strategies for design of delamination specimens are clearly needed.

3.2. Fully-Uncoupled Multidirectional specimens

FUMD delamination specimens were first introduced in [3,4], and allow to concurrently: (i) eliminate all thermoelastic couplings, (ii) have identical properties for all specimen regions (arms and uncracked region), and (iii) freely choose the orientations of the plies embedding the delamination plane. They are

obtained combining three ingredients: (i) quasi-trivial (QT) quasi-homogeneous solutions [17,18], (ii) appropriate orientation choice, and (iii) dedicated superposition rules [19]. QT quasi-homogeneous solutions are sequences defined in terms of generic orientations (i.e., the orientation angles can be chosen freely, what is prescribed is the position of the orientations within the sequence) that allow to obtain laminates with $[B] = [0]$ and $[D] \propto [A]$. By adopting appropriate orientation choices, QT quasi-homogeneous solutions can be used to design fully-orthotropic specimens arms having $[B] = [b] = [0]$, $A_{16} = A_{26} = a_{16} = a_{26} = 0$, $D_{16} = D_{26} = d_{16} = d_{26} = 0$, and $\alpha_{xy}^\varepsilon = \alpha_x^\chi = \alpha_y^\chi = \alpha_{xy}^\chi = 0$. Then, using the superposition rules, these sequences can be combined so that both specimen arms have the same properties and so that their superposition, i.e. the entire specimen, is a fully-orthotropic laminate with exactly the same thermoelastic properties. Preliminary experimental results suggest that FUMD specimens are indeed extremely interesting for IFT characterisation [5].

4. Design of FUMD specimens to evaluate the effects of residual stresses on IFT

FUMD specimens, thanks to their flexibility, may be used to investigate the effects of ply-level residual stresses on IFT. While other options exist [4], we focus on FUMD sequences with three orientations, chosen to be 0° and the generic pair $\pm\delta$. This choice combines design flexibility with simplicity of analysis. For each arm, we indicate with n the total number of plies, with n_0 the number of 0° plies and with n_δ the number of plies at $\pm\delta$; hence $n = n_0 + n_\delta$. As explained, all FUMD specimens have identically null thermoelastic couplings: thus $B_t = 0$ for both specimen arms and for the uncracked region. Also, they have identical thermoelastic properties in the two different arms and in the overall stacking sequence as well. In the following, we consider ply properties as reported in Table 1, comparable with those of a carbon/epoxy UD tape.

Table 1. Ply material properties used for computations.

E_1 (GPa)	E_2 (GPa)	G_{12} (GPa)	v_{12} (-)	α_1 (10-6/°C)	α_2 (10-6/°C)
150	10	5	0.3	0	30

The first aspect to consider in the design is the finite width effect. As explained in Section 2.3, this may be related to the D_c ratio. For FUMD specimens, $[D] \propto [A]$; we can then define the ratio A_c as:

$$A_c = \frac{A_{12}^2}{A_{11}A_{22}}. \tag{8}$$

For FUMD specimens $A_c = D_c$. Hence, A_c can be conveniently used instead of D_c, being much easier to express and compute. Furthermore, for the FUMD specimens considered, all terms in Eq. (8) can be easily expressed explicitly. Introducing the fraction of 0° plies $f_0 = \frac{n_0}{n}$, A_c may be written as:

$$A_c = \frac{(f_0 Q_{12} + (1 - f_0)\bar{Q}_{12}(\delta))^2}{(f_0 Q_{11} + (1 - f_0)\bar{Q}_{11}(\delta))(f_0 Q_{22} + (1 - f_0)\bar{Q}_{22}(\delta))}. \tag{9}$$

Eq. (9) shows that A_c, for the present case, is a function of only δ and f_0 and can be easily computed for the entire set of FUMD specimens under consideration. The value of A_c as a function of δ and f_0 is plotted in Figure 2. Clearly, as the relative number of 0° plies increases and as the value of δ approaches 0°, the value of A_c lowers. On the contrary, when δ moves toward +45° or -45°, A_c increases, and it increases faster for lower values of the fraction of 0° plies, as expected.

Next, ply-level residual stresses should be considered. It was already shown [3,4] that for FUMD specimens $[B] = [0]$, $\{V\} = \{0\}$, $U_{xy} = 0$, and matrices $[A]$, $[D]$, $[a]$, and $[d]$ are all orthotropic and consequently $\alpha_{xy}^\varepsilon = 0$ and $\{\alpha^\chi\} = \{0\}$. Also, since $[B] = [0]$, then $[a] = [A]^{-1}$. From Eq. (3) it follows:

$$\{\alpha^\varepsilon\} = [a]\{U\}, \tag{10}$$

And we can rewrite Eq. (7) as:

$$\{\sigma\} = [\bar{Q}]\Delta T(\{\alpha^\varepsilon\} - \{\bar{\alpha}\}). \tag{11}$$

In Eq. (11), the term inside the parentheses shows once again how ply-level residual stresses are originated from the difference between the contraction imposed on a ply and the contraction it would undergo if not constrained; interestingly, a FUMD laminate contracts only in-plane (and only along the principal directions, since $\alpha^\varepsilon_{xy} = 0$) and the computation of the residual stresses becomes much more straightforward. Indeed, the dependence on the ply position has disappeared (thanks to $\{\alpha^\chi\} = \{0\}$).
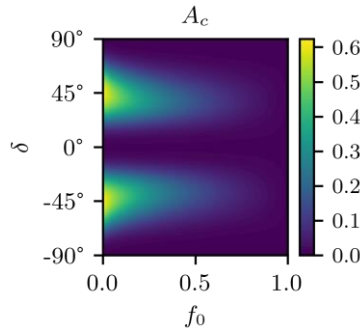

Figure 2. Contour plot of A_c ratio as a function of the angle δ and of the 0° ply fraction f_0.

In Eq. (11), the terms $[\bar{Q}]$ and $\{\bar{\alpha}\}$ depend on material properties and ply orientation; $\{\alpha^\varepsilon\}$, like A_c, is a function of δ and f_0 only. This means all plies having the same orientation will have the same residual stresses. Moreover, we can derive analytical expressions for the ply-level residual stresses, both for the 0° and the $\pm\delta$ plies. Eventually, through a rotation, the stresses in material coordinates can be obtained. Figure 3 shows, for an assumed $\Delta T = -160$ °C, contour plots of the residual stresses in 0° plies as a function of δ and f_0, both in the fibre direction (σ_1) and in the transverse direction (σ_2); it is worth noting that 0° plies in a FUMD specimen will not develop shear residual stress (σ_6). As can be seen, depending on the chosen δ and f_0, significantly different residual stress state can be obtained in 0° plies. Figure 4 shows, again for $\Delta T = -160$ °C, contour plots of the residual stresses in plies at an angle δ as a function of δ and f_0, in the fibre direction (σ_1), in the transverse direction (σ_2) and in shear (σ_6). Once again, significant changes in residual stresses can be obtained choosing different values for δ and f_0. It is also worth noting that transverse and shear stresses may assume, for many configurations, values that are far from negligible when compared to the relative material strengths, especially considering this analysis does not account for micro residual stresses.
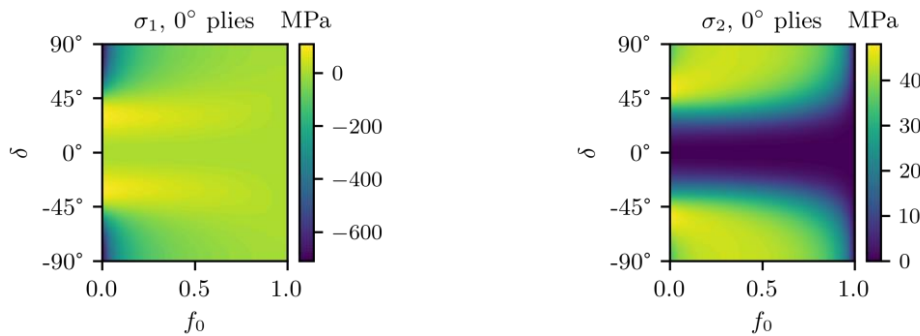

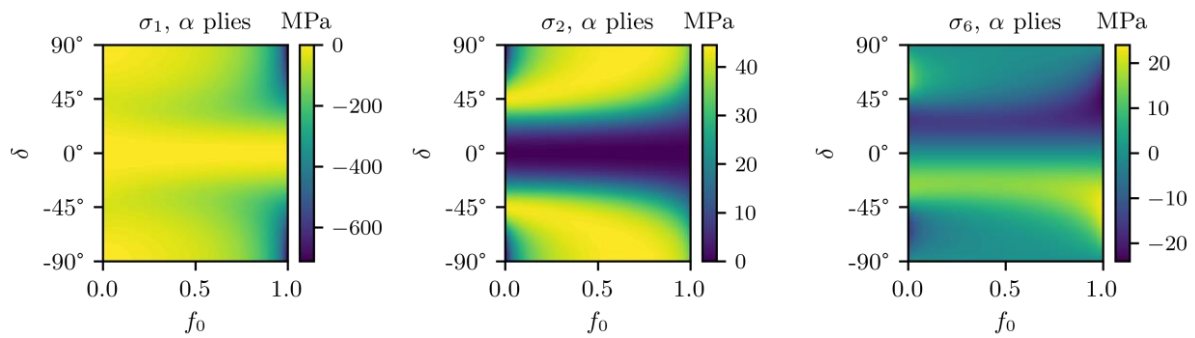**Figure 3.** Contour plots of residual thermal stresses in the 0° plies as a function of δ and of f_0.

Figure 4. Contour plots of residual thermal stresses in the 0º plies as a function of δ and of f_0.

Overall, Figures 2-4 shows how the propension to finite width effect relates to the development of ply-level residual stresses in FUMD specimens of the type studied here. While in the present case, thanks to the properties of FUMD sequences this relationship can be easily derived and presented, for general stacking sequences it would be too cumbersome to analyse.

Hence, making use of the information presented here, it is possible to choose intervals of interest for the parameters δ and f_0 and retrieve FUMD sequences falling within those intervals. This allows to create and analyse a set of specimens to evaluate the effects of ply-level residual stresses.

5. Conclusions

In this work, we reviewed some of the challenges associated with the characterisation of IFT in MD interfaces. We focused on 3D effects and residual thermal stresses. We demonstrated that FUMD delamination specimens, in addition to eliminating all thermoelastic couplings, allow a carefully thought design process and a great control on the laminate propension to finite width effect and on its ply-level residual stresses. Thanks to this, we can design set of FUMD specimens that may allow to study and understand better the effects of ply-level thermal residual stresses on IFT.

References
[1] E. S. Greenhalgh, C. Rogers and P. Robinson. Fractographic observations on delamination growth and the subsequent migration through the laminate. *Composites Science and Technology*, 69(14):2345-2351, 2009.
[2] J. Andersons and M. König. Dependence of fracture toughness of composite laminates on interface ply orientations and delamination growth direction. *Composites Science and Technology*, 64(13–14):2139-2152, 2004.
[3] T. Garulli, A. Catapano, D. Fanteria, J. Jumel and E. Martin. Design and finite element assessment of fully uncoupled multi-directional layups for delamination tests. *Journal of Composite Materials*, 54(6):773-790, 2020.
[4] T. Garulli. Design and validation of Fully-Uncoupled Multi-Directional lay-ups to evaluate interlaminar fracture toughness. Doctoral dissertation, 2020.
[5] T. Garulli, A. Catapano, D. Fanteria, W. Huang, J. Jumel and E. Martin. Experimental assessment of Fully-Uncoupled Multi-Directional specimens for mode I delamination tests. *Composites Science and Technology*, 200:108421, 2020.
[6] P. Prombut, L. Michel, F. Lachaud and J.J. Barrau. Delamination of multidirectional composite laminates at 0°/θ° ply interfaces. *Engineering Fracture Mechanics*, 73(16):2427-2442, 2006.

[7] B. D. Davidson, R. Krüger and M. König. Effect of stacking sequence on energy release rate distributions in multidirectional DCB and ENF specimens. *Engineering Fracture Mechanics*, 55(4):557–569, 1996.

[8] B. D. Davidson and R. A. Schapery. Effect of Finite Width on Deflection and Energy Release Rate of an Orthotropic Double Cantilever Specimen. *Journal of Composite Materials*, 22(7):640-656, 1988.

[9] J. A. Nairn. Fracture mechanics of composites with residual thermal stresses. *ASME Journal of Applied Mechanics*, 64(4):804–810, 1997.

[10] P.T. Gonçalves, A. Arteiro, N. Rocha and L. Pina. Numerical Analysis of Micro-Residual Stresses in a Carbon/Epoxy Polymer Matrix Composite during Curing Process. *Polymers*, 14:2653, 2022.

[11] P.T. Gonçalves, A. Arteiro and N. Rocha. Micro-mechanical analysis of the effect of ply thickness on curing micro-residual stresses in a carbon/epoxy composite laminate. *Composite Structures*, 319:117158, 2023.

[12] T.A. Sebaey, N. Blanco, C.S. Lopes and J. Costa. Numerical investigation to prevent crack jumping in Double Cantilever Beam tests of multidirectional composite laminates. *Composites Science and Technology*, 71(13):1587-1592, 2011.

[13] T.A. Sebaey, N. Blanco, C.S. Lopes and J. Costa. Characterization of crack propagation in mode I delamination of multidirectional CFRP laminates. *Composites Science and Technology*, 72(11):1251-1256, 2012.

[14] R.C. Hudson, B.D. Davidson and J.J. Polaha. Effect of remote ply orientation on the perceived mode I and mode II toughness of θ/θ and $\theta/-\theta$ interfaces. *Applied Composite Materials*, 5:123–138, 1998.

[15] J. A. Nairn. Energy release rate analysis for adhesive and laminate double cantilever beam specimens emphasizing the effect of residual stresses. *International Journal of Adhesion and Adhesives*, 20(1):59-70, 2000.

[16] P. Robinson, S. Foster and J. Hodgkinson. The Effects of Starter Film Thickness, Residual Stresses and Layup on GIc of a 0°/0° Interface. *Advanced Composites Letters*, 5(6), 1996.

[17] P. Vannucci and G. Verchery. A special class of uncoupled and quasi-homogeneous laminates. *Composites Science and Technology*, 61(10):1465-1473, 2001.

[18] T. Garulli, A. Catapano, M. Montemurro, J. Jumel and D. Fanteria. Quasi-trivial solutions for uncoupled, homogeneous and quasi-homogeneous laminates with high number of plies. In *6th ECCOMAS European Conference on Computational Mechanics: Solids, Structures and Coupled Problems, ECCM 2018*, volume 1, pages 255-265, 2018

[19] T. Garulli, A. Catapano, M. Montemurro, J. Jumel and D. Fanteria. Quasi-trivial stacking sequences for the design of thick laminates. *Composite Structures*, 200:614-623, 2018.